Scientific Research and Essays Vol. 7(35), pp. 3114-3127, 6 September, 2012
Available online at http://www.academicjournals.org/SRE
DOI: 10.5897/SRE12.305
ISSN 1992-2248 ©2012 Academic Journals

Full Length Research Paper

Iris recognition system based on video for unconstrained environments

Juan Colores-Vargas[1], Mireya García-Vázquez[1], Alejandro Ramírez-Acosta[2], Mariko Nakano-Miyatake[3] and Héctor Perez-Meana[3]*

[1]CITEDI, National Polytechnic Institute, Av. Del Parque 1310, Tijuana BC. Mexico.
[2]MIRAL R&D, 1047 Palm Garden, Imperial Beach, CA, USA.
[3]ESIME Culhuacan, National Politechnic Institute, Av. Santa Ana 1000, Col. San Francisco Culhuacan, 04430 México D.F. México.

Accepted 27 August, 2012

This paper proposes an iris image quality and segmentation accuracy evaluation method for video-based iris recognition systems, operating in unconstrained environment. Proposed approach consists of two stages of video quality evaluation that allows improving the iris recognition rates in non-ideal or no cooperative situations; where the first stage discards the low quality eye frames, while the second stage discards frames with low quality iris segmentation providing properly segmented iris frames to carry out the unconstrained iris recognition task. Although proposed scheme was evaluated using the Daugman algorithm, it may be used with several other iris recognition systems operating in constrained environments. Evaluation results show that the performance of conventional iris recognition system, using the proposed scheme, reduces the equal error rate (EER) value in about 12.2%.

Key words: Biometric systems, video-based iris recognition, image quality measure, non-ideal iris frames, segmentation accuracy evaluation, unconstrained environments.

INTRODUCTION

Biometric-based recognition systems have been a topic of active research during the last several years, because they allow accurate person identification and identity verification. Among them, the iris recognition systems have received much attention, because they provide high recognition rates besides that the iris characteristics are invariant and their acquisition requires only taking a picture. Most iris recognition systems have been developed to operate in constrained environments (Daugman, 2003; Phillips et al., 2007; Proenca and Alexandre, 2007; Newton and Phillips, 2009), which require the cooperation of the person under analysis to obtain good quality images during the acquisition process. This fact allows conventional iris recognition systems to achieve recognition rates higher than 99% under controlled conditions in which it is possible to obtain focused good quality and frontal iris images. However, the iris recognition rates may significantly decrease if the stated conditions are not satisfied and then the quality of iris images is not good enough, as happens when the system is required to operate in unconstrained environments.

The demands of new biometric security services around the world, requiring that the biometric systems operate in unconstrained environments, have been increasing the difficulty of using conventional iris recognition systems that require focused good quality and frontal images for a correct operation. Because in unconstrained environments these conditions are not satisfied, new approaches must be developed to improve

*Corresponding author. E-mail: hmperezm@ipn/hmpm@prodigy.net.mx/ hperez.meana@gmail.com. Tel/Fax: +52 55 5656 2058.

the iris recognition performance in unconstrained environments. Among these approaches, the video-based eye image acquisition for iris recognition seems to be an interesting alternative (Hollingsworth et al., 2009; Lee et.al., 2009; Wheeler et al., 2008; Matey et al., 2006) because it can provide more information through the capture of a video iris sequences. Besides that, it is a friendly system because it is not intrusive and requires few users' cooperation. However, how to effectively deal with the video iris sequence which has images with different quality due to distortions such as defocus, off-angle, occlusions, etc., still remains as a challenging open problem. To solve this problem, Kalka et al. (2006), Chen et al. (2006) and Belcher and Du (2008) incorporated an iris image quality metrics based on information about the location and intensity of the iris pixels. However, the quality metrics proposed in those works assumes perfect iris image segmentation which in many cases cannot be achieved. Hollingsworth et al. (2009) improve the matching performance using signal-level fusion, taking advantage of the temporal continuity in an iris video sequence to create a single average image from multiple frames, but they suppose an ideal situation, in which bad segmented iris frames are manually discarded, that may limit its application. Another interesting approach is proposed by Matey et al. (2006), which introduced an iris recognition system called Iris on the Move (IOM) based on Near Infrared (NIR) video taken at distance in which the person to be analyzed is moving. However, the eye images extracted from this system suffer from several kinds of noisy effects such as motion blurs, occlusion by eyelid or eyelashes, and unexpected light reflections, etc. Due to that, the recognition rate is about 78% (Matey et al., 2006; Matey et al., 2007) which can be considered low for many practical applications. Jang et al. (2009) proposed a focus assessment method for iris recognition systems based on the wavelet transform and Support Vectors Machine (SVM). Here, the wavelet transforms estimates the focus values using the ratio between the averages of high and low frequency sub-band images. Next, the SVM finds the optimal decision boundary between focused and defocused images using the brightness and focus values as input data. This system, which is proposed for fixed images, has a precision of about 97%. Abhyankar and Schuckers (2009, 2010) proposed an off-angle iris recognition system as well as an iris quality assessment and encoding, based on biorthogonal wavelet networks, which are evaluated using experimentally collected and synthetically generated data. In Abhyankar and Schuckers (2010), the system is evaluated for several off-angles providing a fairly good performance for angles less than 45°, while in Abhyankar and Schuckers (20 09), it is evaluated based on occlusion, contrast, focus and angular deformation. Li et al. (2010) proposed an iris segmentation algorithm, for unconstrained environments, where the iris images are captured at a distance and even on-the-move, which combines the use of a k-means clustering method and an improved Hough transform to estimate the iris limbic boundary. Finally to reduce the number of possible failures, a complementary method that uses skin information is employed. Thus, the detection and elimination of the bad-quality eye frames and non-properly segmented iris frames could help to improve the recognition accuracy and then to reduce the processing time. De Marsico et al. (2010, 2011) proposed an efficient iris segmentation algorithm using pupil localization, as well as pupil-iris limbic boundaries reconstruction. They also introduce some criteria that can be used to determine the quality of segmented iris. Daugman (2007) presented a new method for iris segmentation which detects and models the iris inner and outer boundaries in terms of dynamic contours based on discrete Fourier series expansions of the contour data to define a more precise and flexible iris localization, together with a method to correct the projective deformation of the iris images.

Motivated by the previously discussion, this paper proposes an iris image quality evaluation method for video-based iris recognition systems, which may be used together with most iris recognition systems operating in constrained environments. Proposed scheme consists of two stages of video quality evaluation to improve the iris recognition performance in non-cooperative situations. The novelty of proposed method consists on the use of a global method for objectively assessing the quality of captured eye frames to discriminate those with blurring effect, as a first stage, together with the development of the three different metrics to evaluate the segmentation precision of the pupil-iris limbic boundary as a second stage. The output of the latter stage is a metric value representing a binary decision: correct or incorrect segmentation, based on SVM (Vapnik, 1995). Proposed scheme was evaluated using the Masek iris recognition program (Masek and Kovesi, 2003) which provides an efficient implementation of Daugman (2003) and Wildes (1997) iris recognition algorithms. Experimental results show that the performance of conventional iris recognition system, using the proposed scheme, reduces the equal error rate (EER) value in about 12.2%.

MATERIALS AND METHODS

Traditional iris recognition systems, based on still images, after the iris image acquisition, even if the input images are completely distorted or have a minimum quality, processed to generate a recognition score. However, in general, the recognition result obtained by using low-quality images is not successful, so the entire recognition process must be repeated with a new image until getting a proper result. To reduce this limitation, we propose an efficient iris recognition scheme, based on video sequences, with high performance in unconstrained environments.

The proposed scheme, shown in Figure 1, is based on the conventional iris recognition algorithms (Daugman, 1993; Wildes, 1997) modified to operate with video captured on unconstrained environments, with the inclusion of two quality evaluation stages.

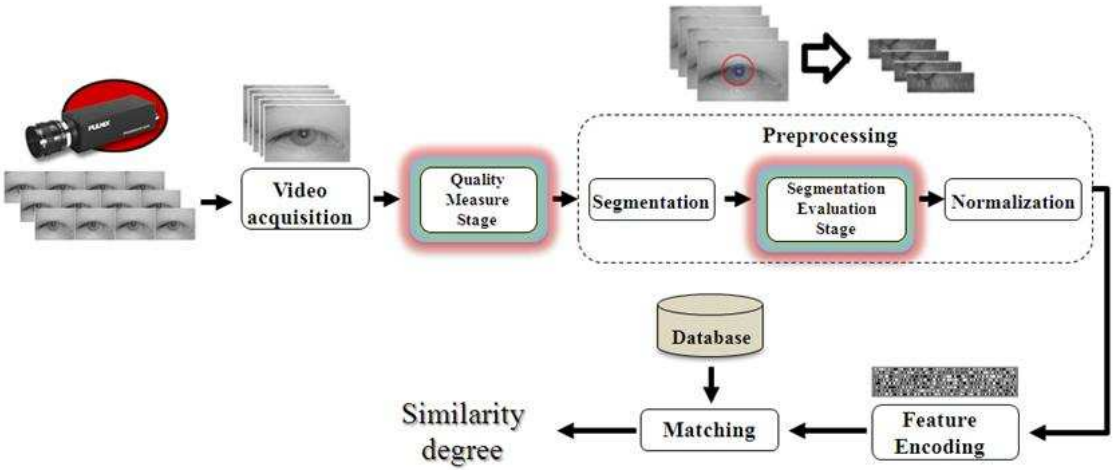

Figure 1. Proposed iris recognition system based on video.

Thus, in the proposed system, firstly, the eye frames are captured by a proper video camera, in the video acquisition stage, which are then feed to a quality measure stage to discard low quality eye frames. Next, if the eye frame under analysis has enough good quality it is fed into a preprocessing module for iris segmentation. It consists of a segmentation stage, based on the Wildes (1997) algorithm which isolates the iris region; a segmentation evaluation stage which determines if the quality of the segmented iris region is good enough for iris recognition or it is necessary to segment a new one; and a normalization stage, based on the Daugman (1993) algorithm, used to compensate the size variation of the iris region. Next, the output of normalization stage is fed into a feature encoding stage (Daugman, 1993) whose output is used, in the matching stage, to provide the similarity degree between the input biometric iris signature and the model stored in the data base. Next, subsections provide a description of each stage.

Video acquisition stage

In all iris recognition system based on video, the main purpose of a video acquisition stage is to capture the video frames with a quality as high as possible. Ideally, the captured eye image should be centered in the frame, free of defocus and aberration errors. It is possible to achieve it by forcing to the user to remain perfectly static and looking to the camera while the video is taken. However, the main purpose of any unconstrained scheme is to be minimally invasive or restrictive with the users. This fact may result, sometimes, in the introduction of frames with few, or even without any iris's texture information, making it necessary to carry out an image quality evaluation, before proceeding with the recognition task, to discard those frames whose distortion renders them not useful for iris recognition.

Quality measure stage

This stage is one of the new elements introduced in the proposed scheme which is applied, after video acquisition, to quickly identify and eliminate the low-quality eye frames that may not be suitable for accurate iris recognition. It is important because reliable image quality estimation may allow discarding the low-quality images improving the iris recognition performance. To discard low quality images is important because we can assume that during the iris video acquisition, not all frames in the sequence are clear and sharp enough for iris recognition. This is because the user to be recognized usually moves his head in different ways giving rise to non-ideal eye frames for recognition tasks, which may include occlusion, off-angle, motion-blur and defocus etc. Defocus-blur and motion-blur are the major source of eye frame quality degradation. Indeed, in a less restrictive environment, the users are free to move outside the optimal distance from the camera during image capture process (Kang and Park, 2005), which means that they may move outside the optimal "depth of field" of the system causing the blurring effects in the images, as shown in the eye frames of Figure 2. Therefore, it is necessary to select suitable eye frames, with enough good quality, from an input video sequence that meet the algorithm's requirements used in the preprocessing module of Figure 1. This stage determines that if the system did not acquire at least one good quality eye frame, the algorithm would activate an indicator to prompt the user to come back and be exposed to the camera again. As shown in Figure 2, choosing an eye frame with an appropriate image quality seems to be a challenge.

In general, a focused eye image has a relatively uniform frequency distribution in the 2D Fourier spectrum, while the power spectrum of a defocused or blurred image is concentrated on the lower frequencies (Daugman, 2004). This fact suggests that a spectral analysis of the frequency distribution, calculating the power spectrum of the higher spatial frequencies, may be an effective way to estimate the image quality of eye frames for discriminating the distorted frames from the clear ones (Daugman, 2004; Wei et al., 2005; Wang et al., 2007; Kang and Park, 2005). Consequently, several discrete formulations have been proposed and that allow obtaining only the power of high frequencies by attenuating the low frequency components of the eye frame and calculating the power spectrum of the highpass filtered eye frame (Daugman, 2004; Wei et al., 2005; Kang and Park, 2005). These methods used to obtain the high frequency power spectrum of the eye frames for image quality assessment, were analyzed by Colores-Vargas et al. (2010). Evaluation results show that the Kang and Park convolution kernel (Kang and Park, 2005) provides better performance than the other kernels in terms of speed and accuracy. Therefore, in the proposed scheme, the quality measure stage employs the Kang and Park convolution kernel. The Kang and Park 5×5 pixels convolution kernel given by Equation 1, consists of the superposition of three square box functions of size 5×5, one function of size 5×5 with amplitude -1, one square function with a segment of size 3×3 centered in (0,0) with amplitude +5, while the remaining elements

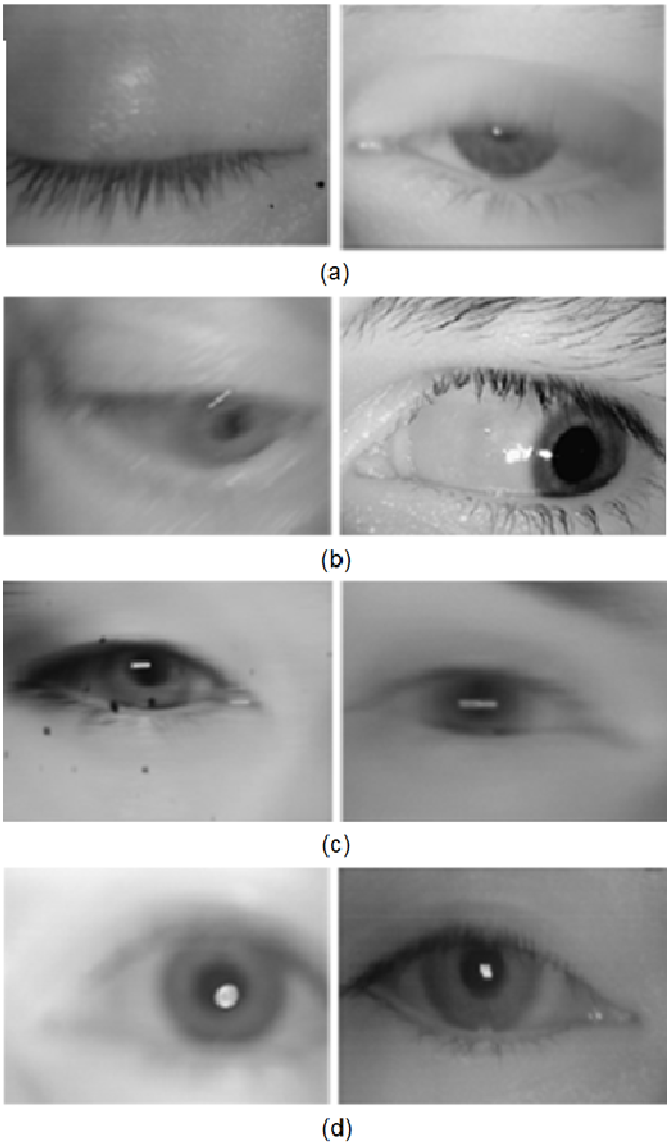

Figure 2. Non ideal eye frames. (a), Occlusion; (b), off-angle; (c), defocus blur; (d), motion blur.

are zero, and one 5 × 5 function in which the coefficients in the positions (-1,-1), (-1,1), (1,-1) and (1,1) have an amplitude equal to -5, while the remaining coefficients are equal to zero (Kang and Park, 2005). The 2D power spectrum of Kang and Park kernel, $K_f(u,v)$, is shown in Figure 3.

$$K(m,n)=\begin{bmatrix} -1 & -1 & -1 & -1 & -1 \\ -1 & -1 & +4 & -1 & -1 \\ -1 & +4 & +4 & +4 & -1 \\ -1 & -1 & +4 & -1 & -1 \\ -1 & -1 & -1 & -1 & -1 \end{bmatrix} \quad (1)$$

Thus, to determine if a given eye image is defocused, firstly it is convolved with the kernel $K(m,n)$ to obtain:

$$c(m,n)=\sum_{r=-2}^{2}\sum_{q=-2}^{2}K(q,r)I(m+q,n+r), \quad m=0,1,2,..N_1, n=0,1,2,...,N_2 \quad (2)$$

and then, using the Parseval theorem the power of the filtered eye image, P, is estimated as follows:

$$P=\frac{1}{N_1N_2}\sum_{u=0}^{N_1}\sum_{v=0}^{N_2}\left|C(u,v)\right|^2 \quad (3)$$

Where $C(u,v)$ denotes the 2D Fourier transform of filtered eye image $c(m,n)$. Next, P is compared with a given threshold given by Th = 15.8247 (Kang and Park, 2005) and if P > Th, the image is consider as focused image otherwise it is classified as a defocused

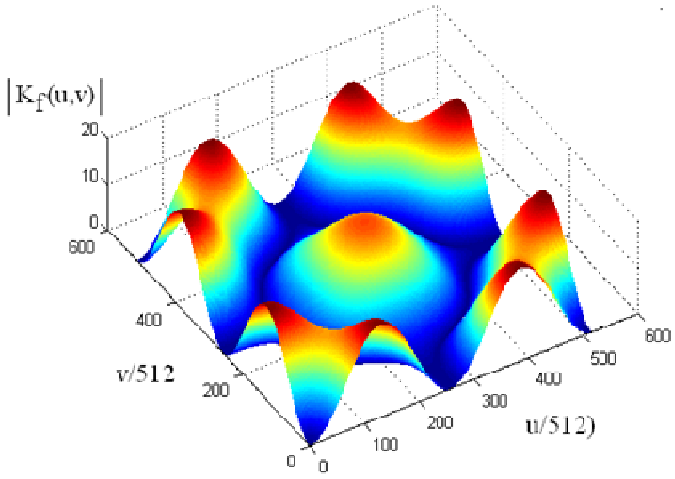

Figure 3. Power spectral density of *K(m,n)*.

eye frame.

Finally, if the quality measure stage classifies the eye frame as a defocused one, it is discarded and a new frame is analyzed, otherwise the eye frame, is fed into a preprocessing module, which consists of a cascade of three stages described, that performs the segmentation, segmentation evaluation (that is, a new element of the proposed scheme) and the normalization processes as shown in Figure 1.

Preprocessing module

The preprocessing module of proposed scheme performs the iris segmentation, segmentation evaluation and normalization tasks whose main purpose is to provide a good enough segmentation of iris region, to enable the encoding and matching stage to perform accurate iris recognition. Next, subsections provide a description of these stages.

Segmentation stage

The segmentation stage isolates the iris region from the eye frames using the segmentation algorithm proposed by Wildes (1997), which is based on the circular Hough transform combined with a Canny edge detector to obtain the iris region. The goal of edge detection algorithms is to produce an image containing only edges of the original image. However, most edge detection algorithms produce an image containing fragmented edges; then in order to turn these fragmented edge segments into useful lines, circles and object boundaries, an additional processing is needed. To this end, the circular Hough transform is used (Wildes, 1997) to find circles in eye frame and deduce the radius $[r_p, r_i]$ and centres $[(x_{cp}, y_{cp}),(x_{ci}, y_{ci})]$ corresponding to the pupil and iris regions according Equations 4 and 5.

$$(x - x_{cp})^2 + (y - y_{cp})^2 = r_p^2 \quad (4)$$

$$(x - x_{ci})^2 + (y - y_{ci})^2 = r_i^2 \quad (5)$$

Segmentation evaluation stage

This stage evaluates the segmentation accuracy to determine if the iris region has been correctly segmented, based on the calculation of three metrics described. This stage plays a very important role because the iris segmentation process is one of the most important factors driving a good recognition performance. That is, if the iris region of the eye frame is successfully localized, a correct recognition will be achieved.

Most iris recognition systems usually implement the segmentation process in the earliest stages; thus, any failure on it compromises the whole recognition process as shown in Figures 4a to 4c. So, if the segmentation process is not performed with enough precision, the segmentation error will further propagate to the encoding and matching steps. So, as a new element of this work, we propose a stage to assess the segmentation accuracy of the iris region. Thus, the inclusion of this segmentation evaluation stage in an automatic iris recognition system may play an important role because, if it is possible to discard the eye frames without the minimum quality required to ensure the recognition of a given user, an important amount of processing for the encoding and matching steps can be avoided.

The proposed method to evaluate the iris segmentation accuracy, shown in Figure 5, is based on the evaluation of three segmentation accuracy metrics. These metrics produce scores that are used as attributes to build a model using a SVM (Vapnik, 1995; Lim et al., 2001), to determine if the segmentation was a success or failure. The model determines if both, the pupil and iris boundaries were correctly estimated (good segmentation) or at least one of the boundaries was incorrectly estimated (failed segmentation) and further describe each one of these segmentation quality metrics.

As previously mentioned, the proposed feature selection scheme is based on the SVM for evaluation of iris segmentation accuracy (Vapnik, 1995; Lim et al., 2001; Fan et al., 2005). We define a vector **X** to describe the segmentation of the iris region in an eye frame, which consists of three values ($\mathbf{X_1}$, $\mathbf{X_2}$, $\mathbf{X_3}$) that reflect different attributes about the segmentation accuracy.

It is important to highlight that each attribute was chosen because it can identify different failures that occur in the segmentation algorithm. Thus, by grouping the three attributes we can generate a novel method to calculate the efficiency of the segmentation process, which is robust to anomalies generated by local problems in the eye frames such as occlusions, off-angle

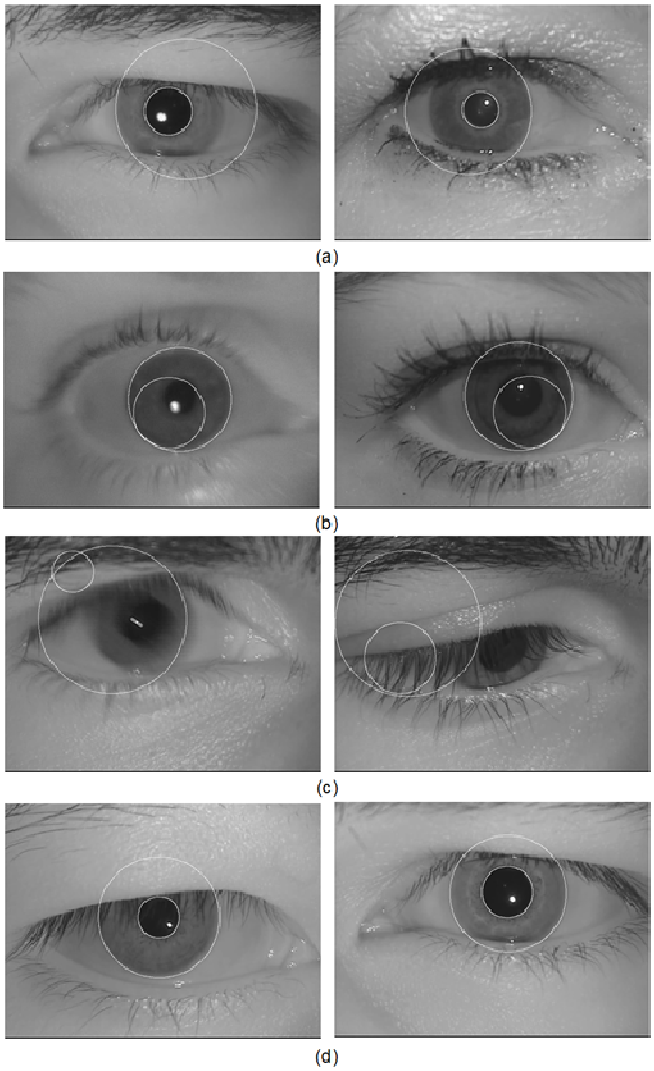

Figure 4. Possible segmentation results; (a), Failed iris segmentation; (b), failed pupil segmentation; (c), failed pupil and iris segmentation; (d), correctly pupil and iris segmented in the eye frame.

and reflections.

For a given vector **X**, the SVM is used to determine if the eye frame is segmented correctly or not. The results provided by this stage are fundamental because if the segmentation is not performed with enough precision, the segmentation error will further propagate affecting the operation of the encoding and matching stages and as a consequence, the iris image will not be useful to carry out the recognition process. Next, a brief description of the calculation of the three metrics which are used to form the segmentation vector **X** is provided.

Attribute X_1 dilatation degree: Consider $\mathbf{X_1}$ to be the metric denoting the dilatation degree (Belcher and Du, 2008), estimated using the radius of the pupil region (r_p) and the radius of the iris region (r_i) for each eye frame provided by the segmentation process. To measure the dilatation degree between the pupil and iris region, the ratio between the pupil radius and the iris radius in pixels given by Equation 6 is computed. Since the pupil radius is always smaller than the iris radius, this dilatation ratio must fall between 0 and 1. Experiments conducted by Belcher and Du (2008) show that the expected values of this metric, when a good segmentation of the iris region is achieved, closely approach a Gaussian distribution with a mean approximately equal to 0.43 and a standard deviation of 0.25. These values were deduced from the results given in Belcher and Du (2008).

$$\mathbf{X}_1 = \frac{r_p}{r_i} \tag{6}$$

According to the eye frames analysis, it was observed that dilatation measure could serve as segmentation evaluator since in most cases, of correctly segmented frames, the radius of the iris is proportional to the pupil radius. This metric is closely related to that

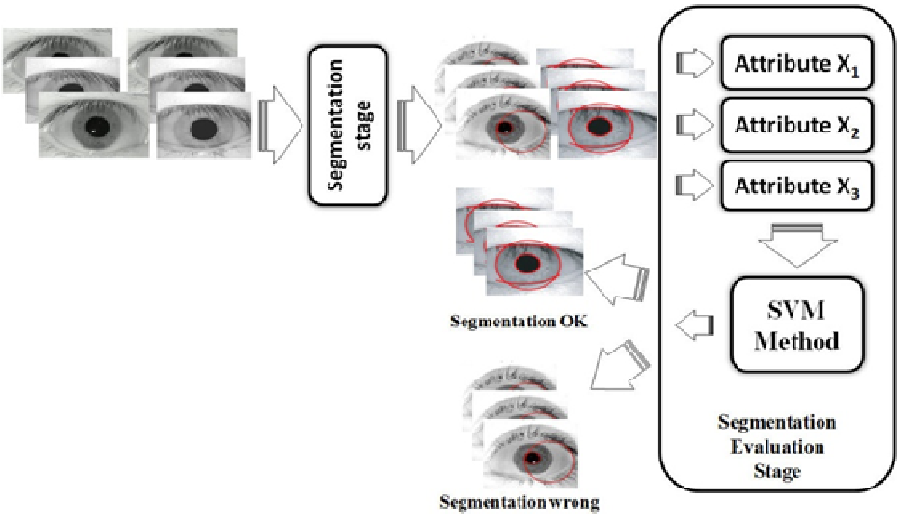

Figure 5. Block diagram of proposed method to evaluate the quality of iris segmentation.

proposed by De Marsico et al. (2011).

Attribute X_2 distance between centers of the pupil and iris: In Proenca and Alexandre (2010), it is mentioned that often the pupil and iris boundaries are not necessarily concentric but the distance between their centers is typically small, with the exception of extreme off-angle images. We observed that when the iris and/or pupil segmentation fail, the distance between the pupil and iris centers increases. According to that, we define the attribute X_2 that measures the distance in pixels between the centers of the pupil and iris, as follows:

$$\mathbf{X}_2 = \sqrt{\left(x_{cp} - x_{ci}\right)^2 + \left(y_{cp} - y_{ci}\right)^2} \quad (7)$$

Where (x_{cp},y_{cp}) and (x_{ci},y_{ci}) are the centre's coordinates of the pupil and iris, respectively.

Attribute X_3 distance separation of distributions: This attribute was proposed after exhaustive experiments where some particular errors were evident when we used only attributes $\mathbf{X_1}$ and $\mathbf{X_2}$. In some cases, the values given by the segmentation algorithm did not correspond to the real location of the iris region; despite the values given by $\mathbf{X_1}$ and $\mathbf{X_2}$ were into the expected range for iris regions correctly segmented. So it was necessary to propose a new attribute based on iris texture rather than proportions. $\mathbf{X_3}$ is a new attribute proposed by our research group as an iris/pupil segmentation measurement, in which we assume that the pupil region of an eye frame is a relatively flat homogenous region of dark intensities respect to the iris region. We also observed that the pixels of the segmented regions that contain an iris and a pupil portion are fitted into Gaussian distributions. The distance separation between both distributions can be calculated using Equation 8, where (μ_p, σ_p) and (μ_i,σ_i) are the mean and standard deviation of the segmented pupil and iris regions, respectively, as shown in Figure 6. In most cases of bad segmented eye frame, the attribute X_3 decrease its value because in the wrong segmented regions, the intensity of its pixels is less homogeneous with respect to the regions taken from a good segmented eye frame. Thus, the value of attribute X_3 indicates the separation between both distributions. Thus, higher distance separation of both distributions, represents better iris segmentation.

$$\mathbf{X}_3 = \frac{\left|\mu_p - \mu_i\right|}{\sqrt{\frac{\sigma_p^2 + \sigma_i^2}{2}}} \quad (8)$$

The normalization process

The normalization process is used to compensate the size variation of the iris region, in the eye frames, mainly because the stretching of the iris caused by pupil dilatation due to varying illumination levels. This process is done using the linear rubber sheet model proposed by Daugman (1993). This transformation maps each point within the iris region to polar coordinates (r,θ) where r and θ are in the intervals [0,1] and [0,2π], respectively. The mapping of the iris region from Cartesian representation $I(x,y)$, to the normalized non-concentric polar representation, $I(r,\theta)$, shown in Figure 7, which is given by

$$I(x(r,\theta), y(r,\theta)) \rightarrow I(r,\theta) \quad (9)$$

Where

$$x(r,\theta) = (1-r)x_p(\theta) + rx_i(\theta) \quad (10)$$

$$y(r,\theta) = (1-r)y_p(\theta) + ry_i(\theta) \quad (11)$$

$$x_p(\theta) = x_{cp}(\theta) + r_p\cos\theta \quad (12)$$

$$y_p(\theta) = y_{cp}(\theta) + r_p\sin\theta \quad (13)$$

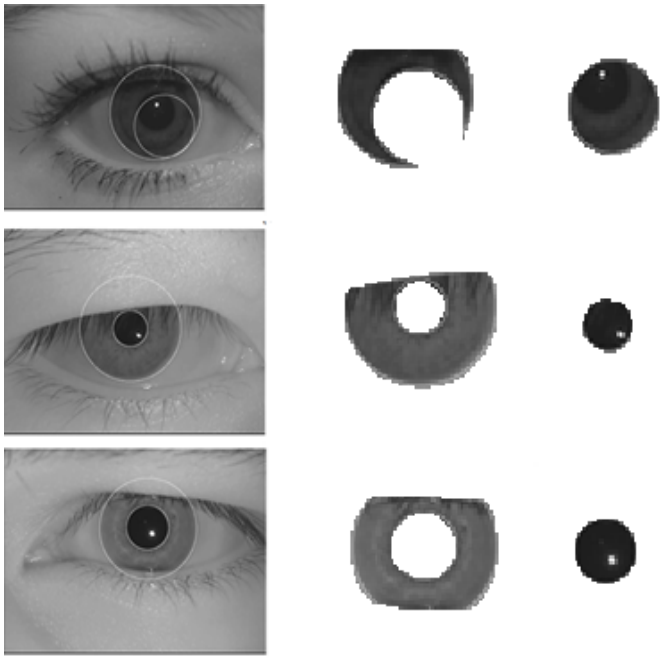

Figure 6. Examples of segmented iris and pupil obtained using Wildes (1997) algorithm.

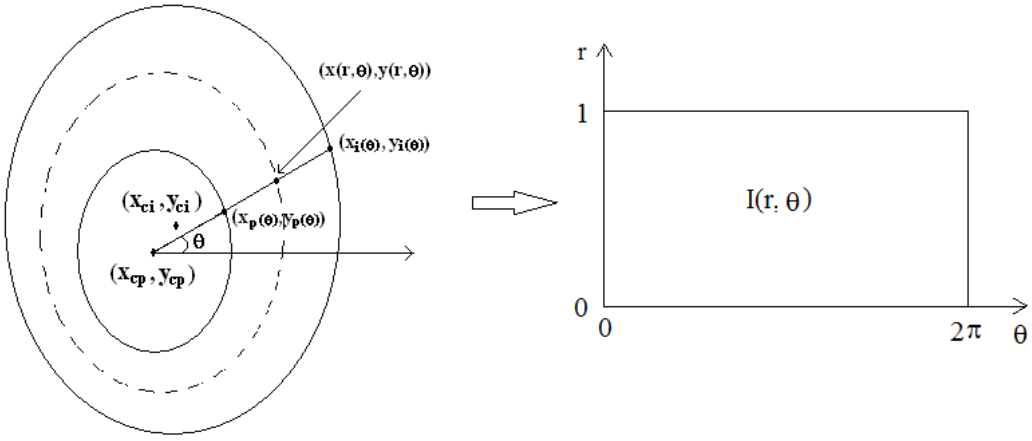

Figure 7. Illustration of normalization procedure.

$$x_i(\theta) = x_{ci}(\theta) + r_i \cos\theta \quad (14)$$

$$y_i(\theta) = y_{ci}(\theta) + r_i \sin\theta \quad (15)$$

$I(x(r,\theta), y(r,\theta))$ is the segmented eye image, (x,y) are the original Cartesian coordinates, *(r, θ)* are the corresponding normalised polar coordinates, (x_p, y_p) and (x_i, y_i) are the coordinates of the pupil and iris boundaries along the radial direction respectively, as shown in Fig. 7; and r_p and r_i are the pupil and iris ratios, respectively.

Feature encoding stage

The extracted features are fed into the encoding stage which is used to obtain the biometric iris signature (Daugman, 2003). This process has two components: firstly, the filter component applied in the normalized iris region using a predefined complex filter or operator to extract the most discriminating information present in an iris region. Secondly, the phase quantization where the resulting complex array is translated into a binary code that constitutes the biometric iris signature. The feature encoding stage, then, was implemented by convolving the normalized iris region with a 1D Log-Gabor wavelets (Daugman, 2003), where each row of $I(r,\theta)$

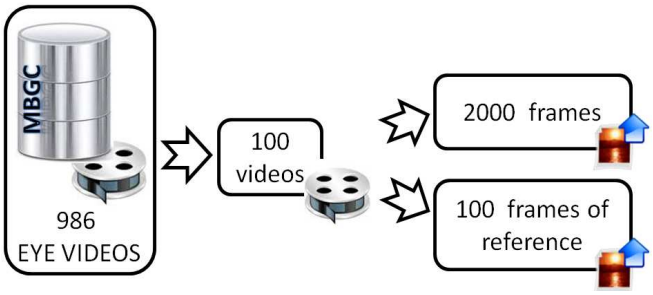

Figure 8. Generation of the testing dataset videos.

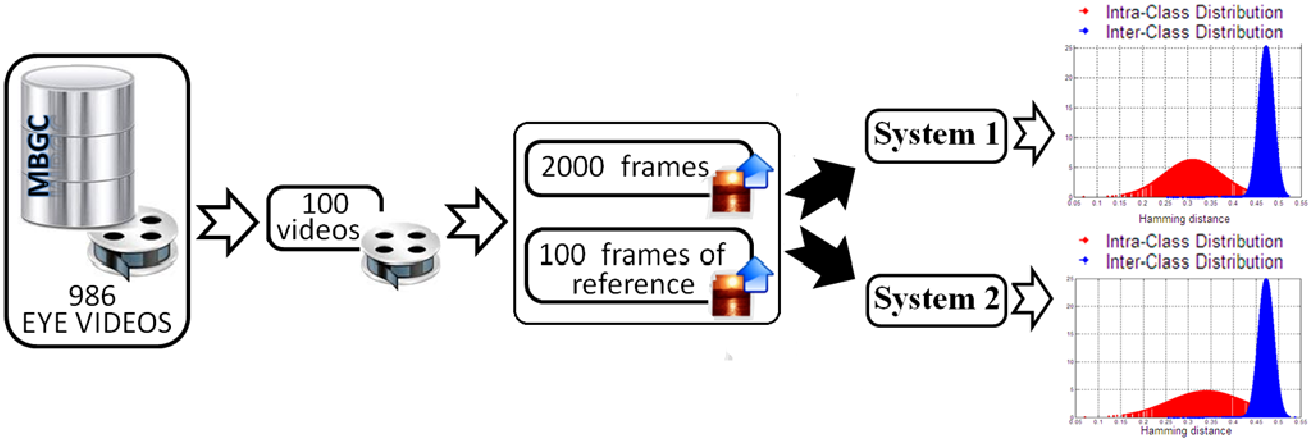

Figure 9. Scenario of the testing systems.

corresponds to a particular circle extracted from the iris rim. Some enhancements are then performed on the extracted signals, such that the intensity values at distorted areas in the normalized iris region are filled with the average intensity of surrounding pixels. Finally, the filter output is transformed into a binary code using the four quadrant phase encoder, with each filter producing two bits of data for each phasor (Daugman, 2003). The encoding stage was implemented using the Masek and Kovesi (2003) program which provides an efficient implementation of this task.

Matching stage

The operation of this stage consists of the comparison of biometric iris signatures, producing each a numeric dissimilarity value. In this scheme, the Hamming distance (HD) that incorporates noise masking was employed (Daugman, 1993). The HD measure can be used to make a decision whether the biometric iris signature is produced by the same or different users. The noise mask helps to use only the significant bits in calculating the HD between two biometric iris signatures.

RESULTS

To evaluate the performance of the proposed scheme shown in Figure 1, we selected the “MBGC.v2” dataset (Phillips et al., 2007), which presents several noise factors, especially those related to reflections, contrast, luminosity, eyelid and eyelash iris obstruction and focus characteristics. Regarding to the images size, each eye frame is 480 by 640 pixels in 8 bits-grayscale at 30 frames per second (fps). This database has been distributed in MPEG-4 format to over 100 research groups around the world. For experiments purposes, 100 videos from the MBGC.v2 database were selected to generate the testing dataset. For each video, we selected 20 frames as testing eye frames and another one as reference eye frame (Figure 8). The testing eye frames were selected randomly, although the reference eye frame was chosen according to the characteristics of high-frequency concentration previously described. The SVM used for segmentation quality evaluation was implemented using the LIBSVM library (Chih-Chung and Chih-Jen, 2011) using a polynomial Kernel type with (gamma*u'*v + coef0)^degree), where coef0 = 1, gamma = 1, cost = 100, and all others parameters are used with their default values given by the LIBSVM (Chih-Chung and Chih-Jen, 2011).

As shown in Figure 9, the recognition tests were conducted on 2000 eye frames with 100 reference eye frames, allowing the generation of the distributions inter-class and intra-class to compare the performance of

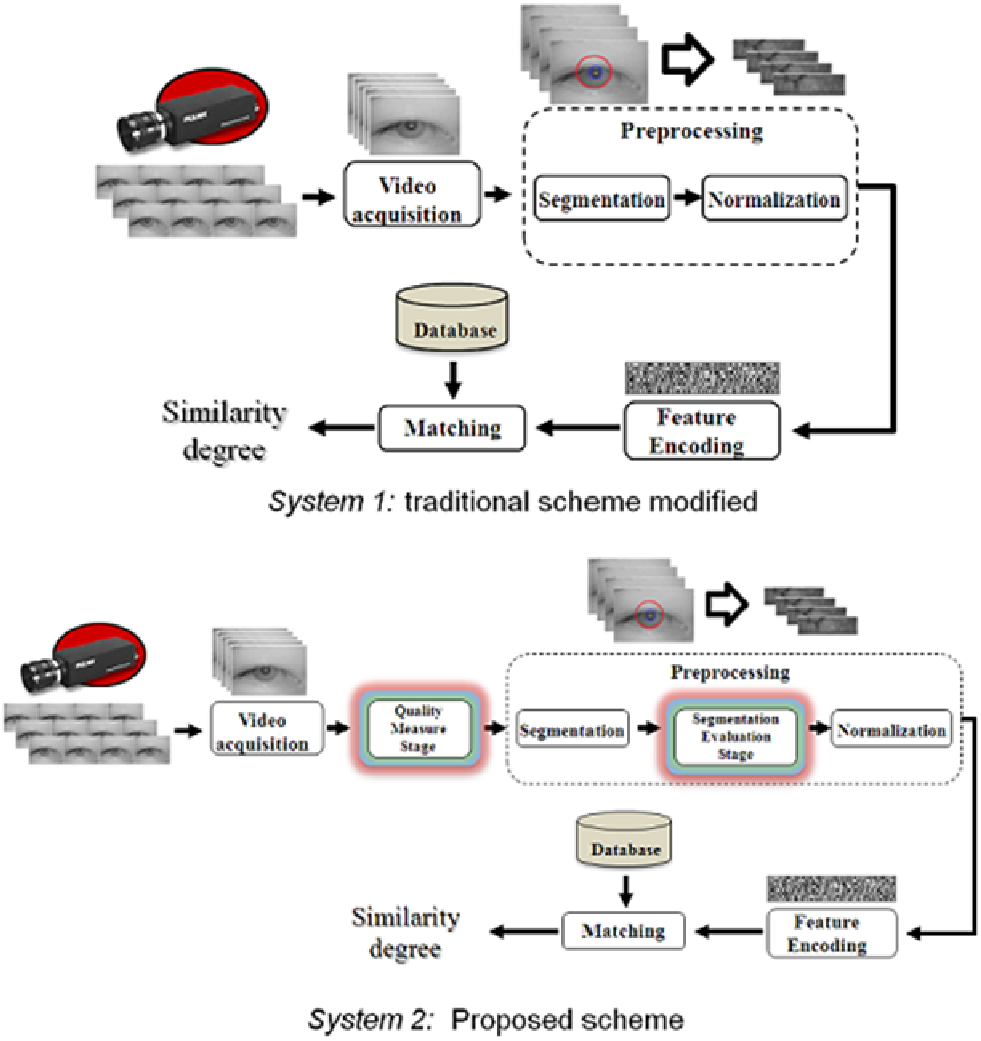

Figure 10. Evaluated systems.

proposed and conventional systems. To evaluate the performance of proposed scheme in verification mode, the EER and the receiver operating characteristics (ROC) curve were used (Zweig and Campbell, 1993).

Figure 10 shows the conventional iris recognition scheme used in constrained environments (Daugman, 1993; Wildes, 1997) modified to process video (System 1) and the proposed scheme called System 2. Figure 11 shows the false acceptance rate (FAR) and false rejection rate (FRR) achieved by System 1 which provides an EER equal to 14.62%, with a threshold (Th) of about 0.457. Figure 12 shows the FAR and FRR achieved by proposed scheme (System 2) which achieves an EER equal to 2.48% with a Th equal to about 0.438. The inner graph in Figures 11 and 12 corresponds to a zoom of the region surrounding the ERR points. The ROC curves, shown in Figure 13, plot the FRR as a function of the FAR are useful to compare the performance of proposed and conventional systems.

Table 1 shows the comparison results of the evaluated video-based iris recognition systems under several situations. In the first case, both systems operates with the same threshold, which was selected randomly; in the second one, the Th is selected such that both systems achieve the same FAR and finally the thresholds are selected such that both systems achieves their respective ERR.

The performance of proposed method to evaluate the quality of segmented iris frames was estimated using 1000 segmented iris frames, among them 698 wrong segmented iris frames and 302 correctly segmented iris frames. Table 2 shows that proposed method classified correctly 990 of such segmented images, that is, 99% of the segmented images under analysis were correctly classified. Finally, the genuine acceptation rate (GAR) for the System 1 is 83.3% while for the System 2 it is about

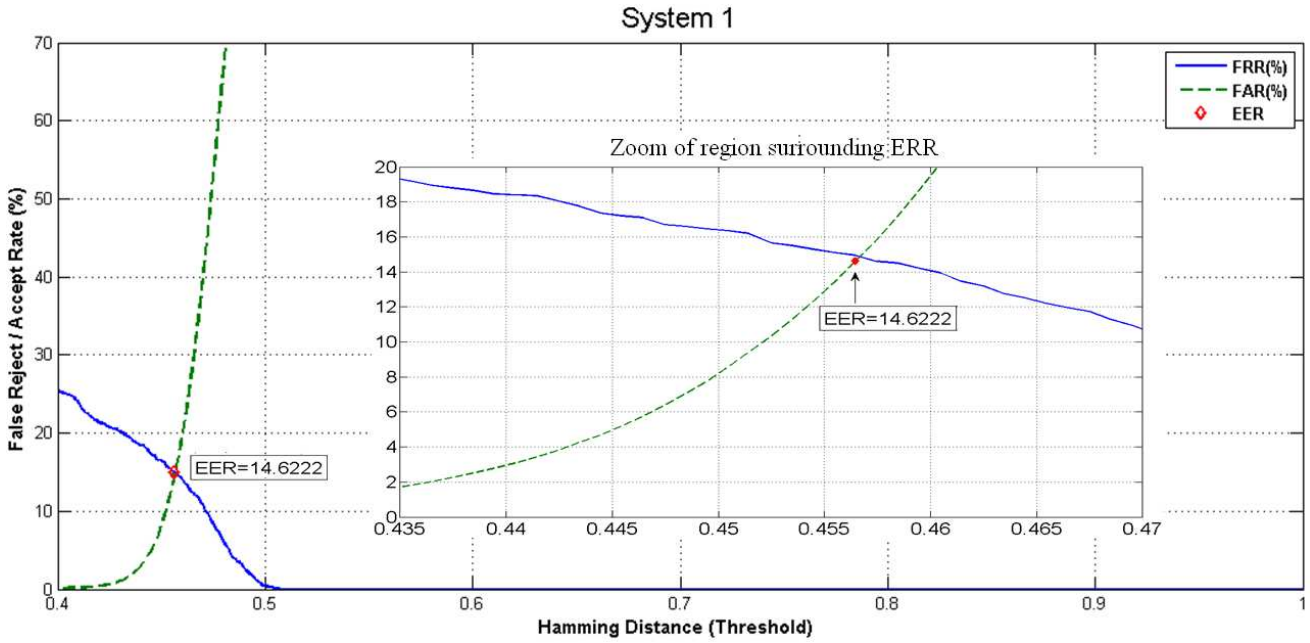

Figure 11. The crossover point between the curves FRR and FAR. EER for System 1.

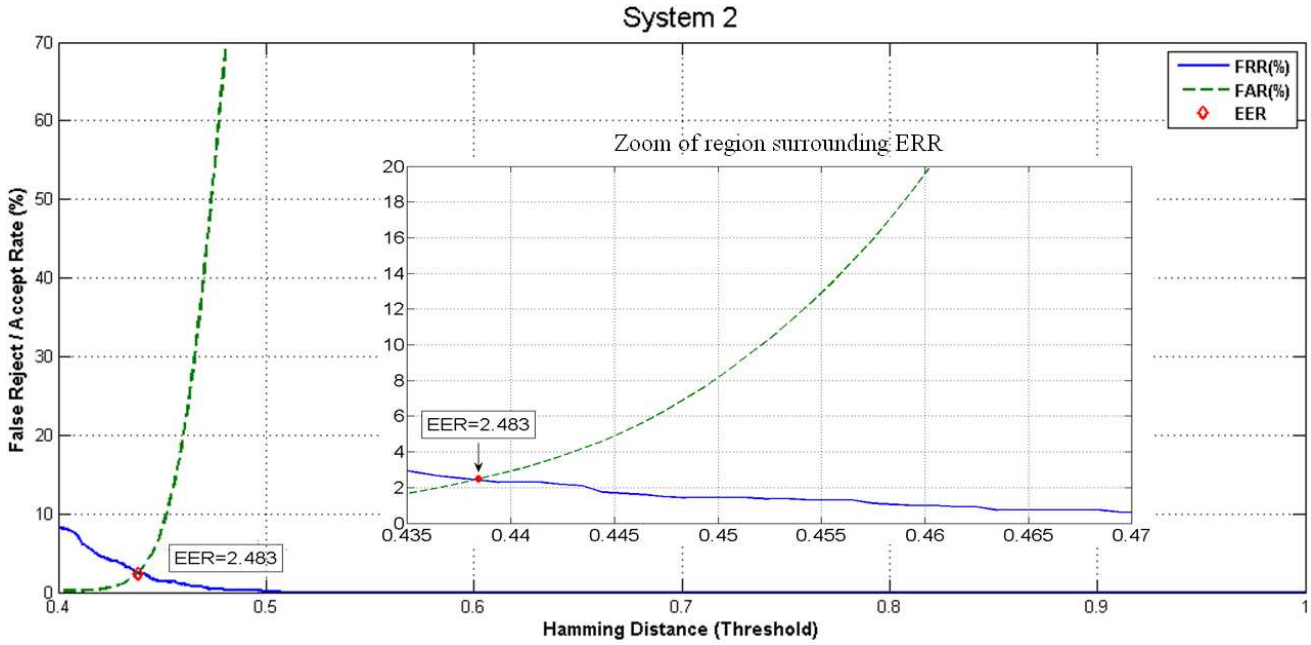

Figure 12. The crossover point between the curves FRR and FAR. EER for System 2.

to 97.34% using Th = 0.44.

DISCUSSION

An important evaluation of any identity verification system consists in determining the point in which the FAR and FRR have the same value, which is called EER, because it allows the user to determine the appropriate Th, for a given application. Thus, if a FAR smaller than ERR is required, a smaller Th in terms of the HD must be used, otherwise a larger Th may be used. Evaluation results

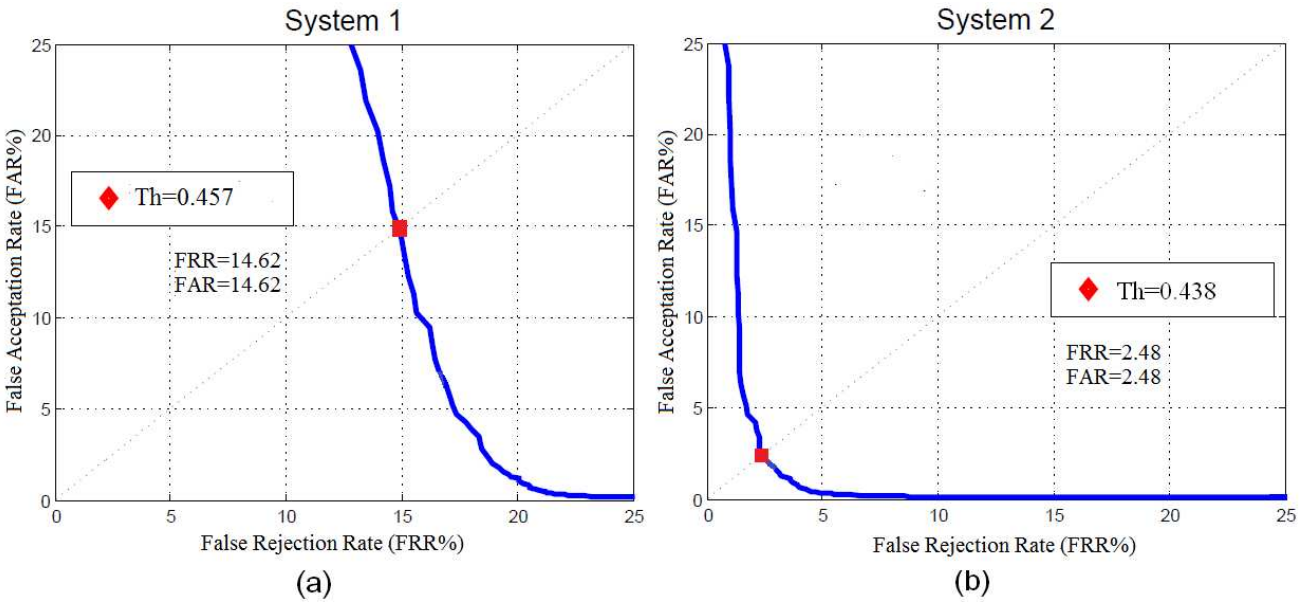

Figure 13. ROC curves together with EER threshold value. (a), System 1; (b), System 2.

Table 1. Overall results generated by System 1 and System 2.

System 1			System 2		
FRR (%)	**FAR (%)**	**Th**	**FRR (%)**	**FAR (%)**	**Th**
18.60	3.10	0.440	2.10	2.51	0.440
19.10	2.00	0.436	2.90	2.00	0.437
14.62	14.62	0.457	2.48	2.48	0.438

Table 2. Classification performance of proposed segmentation quality evaluation method.

Iris frame type	Expected	Estimated	Rate (%)
Wrong segmented	698	690	98.85
Correctly segmented	302	300	99.33

show that proposed scheme significantly improves the performance of conventional iris recognition algorithms, providing and EER = 2.48%, while the conventional scheme achieves an EER = 14.62%. That is, a reduction of about 12.14%. This FAR, that is FAR = 2.48%, can be achieved using the conventional system although in this situation the FRR becomes about 19%. To confirm the accuracy of iris matching process and to show the overall performance of proposed scheme, independently of the threshold value, the ROC curves were used, which plot the FAR as a function FRR. From experimental curves, it follows that the proposed system provides a better performance since the ROC of proposed system is much closer to the origin than the conventional one. Finally, using properly selected Th, that, 0.44, the System 1 may achieve a FAR equal to 3.10%, which is significantly slower than the EER, although in this situation the FRR increases to 18.6% which is much higher than the EER. On the other hand, using the same threshold, the proposed scheme achieves a FAR equal to 2.10% and a FRR equal to 2.51%. In addition, in this situation, the GAR for System 1 is 83.3% while for the proposed system is about to 97.34%.

Regarding the performance of segmentation quality evaluation stage, proposed scheme achieves a correctly evaluation rate equal to 99%, that is, 98.85% of correctly segmented image and 99.33% of wrongly segmented image were correctly classified. This performance

appears to be good enough for most practical applications; however, it may be improved incorporating the segmentation quality evaluation criteria proposed by De Marsico et al. (2011). Thus, instead of using a SVM with 3 inputs and 2 outputs, a SVM with 5 or more inputs and 2 outputs may be used. Also proposed scheme can be used together with other recently proposed segmentation algorithms with eye image restoring capabilities (Daugman, 2007; Proenca and Alexandre, 2010).

Finally, assuming that in a real unconstrained iris recognition system a given person spends 1 s to cross through the detection area, and that only 1/3 of this time is inside the camera capture region, because the camera operates to 30 frames/s, the image acquisition stage only will be able to capture 10 eye images. Thus, since in general only about 35% of those images can be correctly segmented in a single run, there will be available only 3 or 4 images suitable to carry out the recognition task. However, because the proposed scheme achieves a classification rate of about 99%, we can conclude that it can be used in most practical applications requiring unconstrained iris recognition tasks.

Conclusions

In this work, we propose an improved iris recognition system based on video, integrating two evaluation stages into the conventional iris recognition system, in order to increase its adaptability toward less constrained environments. Indeed, under less constrained environments, it is expected that the captured eye frames contain several types of noise and distortion, such as frames with high levels of defocus and motion blur, which affect the segmentation process and consequently impacts the recognition rate. Due to this, the predominant noisy and bad segmented eye frames are discarded by the proposed image quality evaluation and segmentation evaluation stages. The experimental results show that the proposed quality and segmentation evaluation stages help to reduce the recognition error rates contributing to improve the recognition performance. It also decreases the EER by 12.14%; and for a given Th, FAR is reduced by 1.00%, while the FRR is reduced by 16.5% comparing with the traditional iris recognition system. In addition, the GAR achieved by the proposed scheme is 97.34%; while for the conventional system is 83.3%. The proposed scheme seems to be appropriate for non-cooperative iris recognition applications, in which the ability to deal with noisy and distorted eye frames is required.

Regarding the performance of segmentation quality evaluation stage, proposed scheme achieves a correctly evaluation rate equal to 99%. This performance may be good enough for most practical unconstrained environment; however, it may be improved incorporating some other segmentation quality evaluation criteria previously mentioned or using some other segmentation algorithms recently proposed.

ACKNOWLEDGEMENTS

We thanks go to the National Science and Technology Council of Mexico (CONACyT) and to the National Polytechnic Institute of Mexico for the financial support provided during the realization of this research.

REFERENCES

Abhyankar A, Schukers S (2009). Iris quality assessment and bi-orthogonal wavelet based encoding for recognition. Pattern. Recognit. 42:1878-1894.

Abhyankar A, Schukers S (2010). A novel biorthogonal wavelt network system for off-angle iris recognition. Pattern. Recognit. 43:987-1007.

Belcher C, Du Y (2008). A selective feature information approach for iris image quality measure. IEEE Transaction on Inform. Forensics Secur. 3(3):572-577.

Colores-Vargas J, García-Vázquez M, Ramírez-Acosta A (2010). Measurement of defocus level in iris images using convolution kernel method. Lect. Notes Comput. Sci. 6256:164-170.

Chen Y, Dass S, Jain A (2006). Localized iris quality using 2-D wavelets. Proc. of Advances in Biometrics, Int. Conf. Biom. Hong Kong, China 1:373-381.

Chih-Chung C, Chih-Jen L (2011). LIBSVM: a library for support vector machines. http://www.csie.ntu.edu.tw/~cjlin/libsvm.

Daugman J (1993). High confidence visual recognition of persons by a test of statistical independence. IEEE Trans. Pattern. Anal. Mach. Intell. 15(11):1148-1161.

Daugman J (2003). The importance of being random: statistical principles of iris recognition. Pattern Recognit. 36:279-291.

Daugman J (2004). How iris recognition works. IEEE Trans. Circuit Syst. Video Technol. 14(1): 21-30.

Daugman J (2007). New methods in iris recognition. IEEE trans. Syst. Man Cybern. Part B. 37(5):1167-1175.

De Marsico M, Nappi M, Riccio D (2010). IS_{IS}: Iris segmentation for identification systems. Int. Conf. Pattern Recognit. 1:2857-2860.

De Marsico M, Nappi M, Riccio D, Wechsler H (2011). Iris segmentation using pupil location, linearization and limbus boundary reconstruction in ambient intelligent environments. J. Ambient Intell. Human Comput. 2:153-162.

Fan R, Chen P, Lin C (2005). Working set selection using the second order information for training SVM. J. Mach. Learn. Res. pp. 1889-1918.

Hollingsworth K, Peters T, Bowyer KW, Flynn PJ (2009). Iris recognition using signal-level fusion of frames from video. IEEE Transa. Inform. Forensics Secur. 4(4):837-848.

Jang J. Ryoung PK, Kim J, Lee Y (2009). New Focus assessment method for iris recognition systems. Pattern Recognit. Lett. 29:1759-1767.

Kalka N, Zuo J, Schmid N, Bojan C (2006). Image quality assessment for iris biometric, Biometric Technology for Human Identification III. SPIE 6202:D1-D11.

Kang B, Park K (2005). A study on iris image restoration. Lect. Notes Comput. Sci. 3546:31-40.

Lee Y, Phillips P, Michaels R (2009). An automated video-based system for iris recognition. Proc. Int. Conf. Biom. pp. 1-8.

Li P, Liu X, Song X (2010). Robust and Accurate iris segmentation in very noisy iris images. Image Vis. Comput. 28:246-253.

Lim S, Lee K, Byeon O, Kim T (2001). Efficient iris recognition through improvement of feature vector and classifier. ETRI J. 23:61-70.

Matey J, Ackerman D, Bergen J., Tinker M (2007). Iris recognition in less constrained environments. Advances in Biometrics: Sensors, Algorithms Syst. Springer pp. 107-131.

Matey J, Naroditsky O, Hanna K, Kolczynski R, LoIacono D, Mangru S, Tinker M, Zappia T, Zhao W (2006). Iris on the MoveTM: Acquisition of images for iris recognition in less constrained environments. Proceed. IEEE. 94(11):1936-1946.
Masek L, Kovesi P (2003). MATLAB source code for a biometric identification system based on iris patterns. The University of Western Australia.
Newton EM, Phillips PJ (2009). Meta-analysis of third-party evaluations of iris recognition. IEEE Trans. Syst. Man Cybern. Part A. 39(1):4-11.
Phillips PJ, Scruggs W, Toole A, Flynn P, Bowyer K, Schott C, Sharpe M (2007). FRVT 2006 and ICE 2006 large-scale results. Technical Report, Natl. Instit. Stand. Technol. NISTIR p. 7408.
Proenca H, Alexandre L (2007). The NICE.I: Noisy Iris Challenge Evaluation. Proc. of the IEEE First International Conference on Biometrics: Theory Appl. Syst. 1:1-4.
Proenca H, Alexandre L (2010). Iris recognition: analysis of the error rates regarding the accuracy of the segmentation stage. Image Vis. Comput. 28:202-206.
Vapnik V (1995). The nature of statistical learning theory, Springer-Verlag New York, Inc., New York, NY, USA.
Wang J, Xiafu H, Pengfei S (2007). An iris image quality assessment method based on Laplacian of Gaussian operation. IAPR Conf. Mach. Vis. Appl. 1:248-251.
Wei Z, Tan T, Sun Z, Cui J (2005). Robust and fast assessment of iris image quality. Lect Notes Comput. Sci. LNCS 3832:464-471.
Wheeler F, Perera A, Abramovich G, Bing Y, Tu P (2008). Stand-off iris recognition system. Proc. IEEE Int. Conf. Biom. Theory, Appl. Syst. 1:1-4
Wildes R (1997). Iris recognition: an emerging biometric technology. Proceed. IEEE 85(9):1348-1363.
Zweig M, Campbell G (1993). Receiver-operating characteristic (ROC) plots: a fundamental evaluation tool in clinical medicine. Clin. Chem. 39:561-577.